

Two-Stage Three-Phase Power Generation of PV System Using Adaptive Sunflower MPPT Algorithm

Dr.S.Selvakumaran¹, Dr.K.Baskaran²,N.Saranya³

¹ Assistant Professor/EEE Department – Roever Engineering College, Perambalur*

² Professor and Head/EEE Department - Alagappa Chettiar Government College of Engineering and Technology, Karaikudi

³ Assistant Professor / EEE Department – Roever Engineering College, Perambalur

Abstract

The grid-connected photovoltaic system (GCPVS) has challenges such as excessive active power and poor Maximum Power Point Tracking (MPPT) performance. During peak power generation periods, excessive active power can cause overvoltage problems at common coupling points of low or medium voltage grids. Furthermore, improper MPPT technology performance can result in system loss due to the long retention time during irradiation sudden change. As an outcome, in order to solve the power surplus problem, the active power should be reduced using an ASF (Adaptive Sunflower) MPPT algorithm in a collection of various situations. The spatial vector orientation is used in the ASF process to enhance the efficiency of the MPPT algorithm. As a result, the proposed control scheme, which involves an intermediate boost converter, reduces excess active power during peak generation. Furthermore, rather than interacting with peaks, the modified MPPT algorithm deals with insolation fluctuations over time. As a consequence, the proposed control scheme results in a more efficient system during peak power generation. When changing the amount of solar radiation during low usage times, it also reduces power loss and time for settling. The proposed control scheme has been evaluated in MATLAB/Simulink on a 30kW system under various environmental conditions.

Keywords - Grid connected photovoltaic system, maximum power point tracking, adaptive sunflower, voltage source inverter.

1. INTRODUCTION

Excessive use of natural resources over the last few decades has led to rapid depletion of fossil fuels [1] and severe environmental degradation [2], inevitably leading to the destruction of ecosystems and the acceleration of the universal energy crisis [3]. As a result, the energy revolution and transformation are essential to social and economic development [4] and are consistent with the global strategy for sustainable development [5]. Obviously, the development and usage of new energy sources and renewable energy [6] such as solar energy [7] and wind energy [8] are vital and have piqued the interest of people all over the world [9]. Solar energy, in particular, is regarded as one of the most effective alternatives [10, 11]. Solar energy is the ultimate source of energy, and it is referred to as "renewable energy" or "sustainable energy" because it can be replenished naturally in a tiny interval. Because of the severity of the global energy crisis and pollution, photovoltaic systems have identified as a prominent source of energy from renewable sources. Solar power has the largest reserves, an endless supply, and no geographical barriers, making solar energy technology a hot research topic.

The utilisation of solar panels has been steadily increasing recently, due to improvement in solar energy efficiency and the advancement of industrialization technology. Many countries have assembled a large number of solar cell modules on the public power grid in recent years [13]. Solar energy systems can convert solar panels under the influence of sunlight into electrical energy quickly. The conversion efficiency, however, is low, and the energy cost is high. Solar energy has low fuel costs, no pollution, and requires little upkeep. Photovoltaic systems have massive benefits, including increased functionality [14].

The aim of this paper is to provide a thorough investigation of a three-phase load/network system powered by a solar light source. The MATLAB /simulation link is used to implement the solar system simulation model that employs the MPPT algorithm. For maximum power extraction, the system supports MPPT technology. This paper compares the performance of a PV-based three-phase grid/pump system with the proposed ASF MPPT technique to P&O and IC techniques under various weather conditions.

1. At peak power, the ASF technology is proposed to limit power transmission and solve the PCC overvoltage problem.
2. The proposed method for limiting power transfer.
3. This MPPT algorithm improves tracking speed and power loss efficiency under varying irradiation conditions.

2. CONTEXT AND WORK STRATEGY

In this section, the GCPVS system architecture and proposed control mechanism are summed up. The proposed process is divided into two levels, shown in Figure 1.

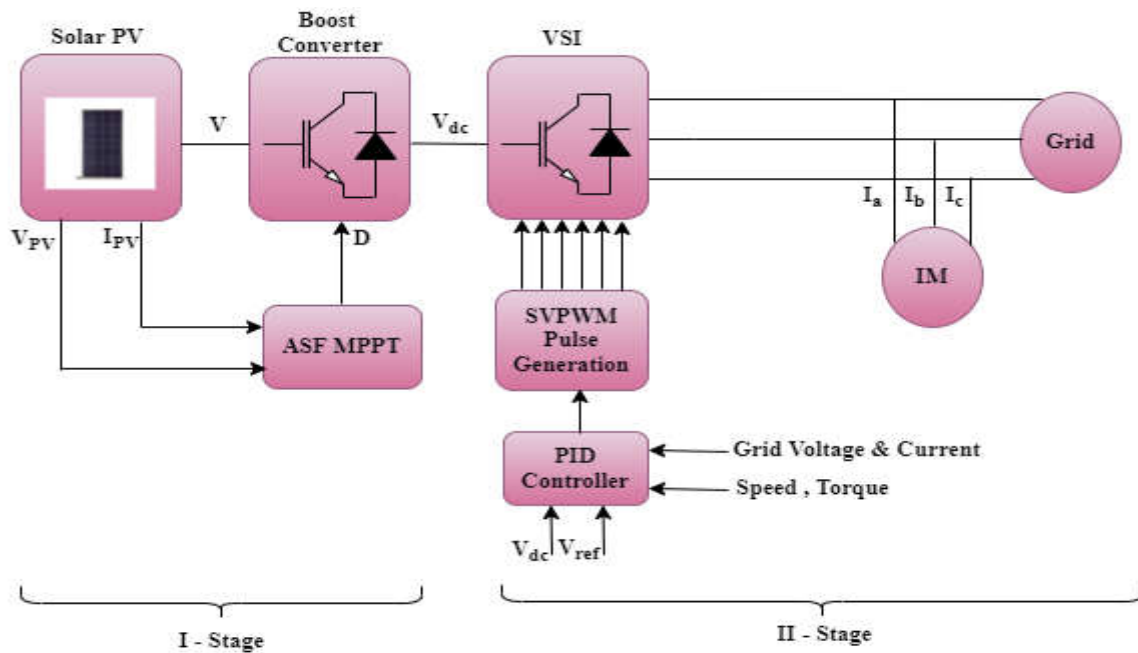


FIGURE 1 Block diagram of two stage three phase PV system

The solar array, boost converter, and MPPT control comprise the first stage. To connect photovoltaic systems to the grid, three-phase VSIs are commonly used. The system's second step consists of an IGBT-based VSI integrated with the system/load. SVPWM for three-phase VSI can provide reasonably close switching patterns, reducing switching device stress and losses and enhancing line current waveforms [16-17]. Solar energy system utility interface standards, such as power quality, safety, and protection functions, are complied with IEEE 929-2000[18]. Grid-connected inverter control strategies are currently playing a key role in delivering high-quality power to the grid. Grid-connected three-phase photovoltaic systems can benefit from current-controlled SVPWM inverters [16,19,20-21]. Finally, the entire system is designed and simulated for a 30kW, two-level, and three-phase photovoltaic system that are integrated into the network.

3. CONTROL TECHNIQUE PROPOSED - ADAPTIVE SUN FLOWER (ASF)

Over time, the proposed correction algorithm reduces power loss and improves response. It also keeps the system from drifting under different irradiation conditions. Furthermore, the proposed MPPT controls various Optimal Power Flow (OPF) scenarios and limits the generation of excess power during peak hours. The main driving force behind the use of ASF algorithms to solve these optimization problems is the evolution of soft-computing optimization algorithms. Nature inspired this algorithm. The ASF algorithm simulates the movement of sunflowers in order to capture solar radiation.

The sunflower flower's behaviour is to find the best direction towards the sun. Every morning, repeat the sunflower cycle. They stood up and began their day by following the sun. They still wait for the next sunrise and move in the opposite direction at the end of the day. It is critical to have a copy of the inverse square law. Sunflowers receive much more heat than places further away and tend to settle in the area because they are closer to the sun. Sunflowers, on the other hand, are less susceptible to heat and go to greater lengths to get as close to the sun's sweet spot as possible [22]. The amount of calories received by each population is represented by Equation (1).

$$Q_i = \frac{P}{4\pi r_i^2} \quad (1)$$

Where P denotes the source's power and r_i denotes the distance between the optimal current and population i. The algorithm's moisture content is determined at random based on the shortest distance between flower i and flower i+1. In fact, piebald emits a large number of pollen mates. To make the algorithm easier to understand, assume that each sunflower produces a pollen mate and replicates itself. The equation is the sunflower's direction to the sun (2)

$$\vec{s}_i = \frac{X^* - X_i}{\|X^* - X_i\|}, i=1,2,...n_p. \quad (2)$$

The phase of sunflower is expressed as "s" in Equation (3)

$$d_i = \lambda \times P_i (X_i + X_{i-1}) \times \|X_i + X_{i-1}\| \quad (3)$$

Where λ is a constant defining the plant's "inertial" displacement. The probability of moisture is given by $P_i (\|X_i + X_{i-1}\|)$. To produce new sunflowers in the new location, the sunflower is moistened with another nearby sunflower. The distance between the flowers determines this new position. The closer you are to the sun, the fewer steps you must take to find local improvements. The rest of the people in the room moved normally. These steps are subject to some constraints in order to prevent people from exceeding the search space specified in the equation (4)

$$d_{\max} = \frac{\|X_{\max} - X_{\min}\|}{2N_{\text{pop}}} \quad (4)$$

Where X_{\max} and X_{\min} are the upper and lower bounds, respectively, and N_{pop} is the population size.

$$\vec{X}_{i+1} = \vec{X}_i + d_i \vec{s}_i \quad (5)$$

The algorithm first creates a random or uniform population. The highest rated population is the one that transforms under the sun. So these people turn themselves to the sun and take random steps in a fixed direction. The proposed system implements an ASF MPPT algorithm. SFOA is extremely sensitive to two parameters: moisture rate (P_r) and mortality (m). This heightened sensitivity does not guarantee the discovery of the best sunflowers. Furthermore, each sunflower's inertial displacement is defined as a constant, limiting the SFOA search operation. These two constraints do not lend themselves to SFOA study navigation. This paper proposes two modifications to address the aforementioned limitations. The first change suggests converting the moisture content (P_r) from the specified constant value to the next adaptive value.

$$P_r = (1 - \frac{w}{\max_w}) \quad (6)$$

This equation is described as a linear equation that iteratively reduces the coefficient vector (P_r) from 1 to 0. The second modification demonstrates that the inertial displacement (D_s) creates an adaptive description for each sunflower, as illustrated in (8).

$$D_s = (t - b) * \left(1 - \frac{w}{\max_w}\right) \quad (7)$$

The minimum and maximum constraints of the decision variables are distinguished by t and b . The current iteration is denoted by w . During peak hours, the PV array generates excess power. As a result, in order to remove the excess power, a power limit must be set within which the power can be transferred without affecting the distribution network equipment. In this paper, a power limit P_{limit} , which is the average of power generated from 9 to 16 hours of the day, is considered and presented as follows.

$$P_{\text{limit}}(t) = \frac{P(t_8) + P(t_9) + \dots + P(t_{17})}{t_8 + t_9 + \dots + t_{17}} \quad (8)$$

ASF ALGORITHM

Step 1: Begin

Step 2: Define the Starting Conditions

Step 3: Create the initial population with values within the specified range.

Step 4: Calculate the value P_{pv} for each duty cycle

Step 5: Determine the orientation of the spatial vector.

Step 6: Remove the most $m\%$ plants.

Step 7: Revise P_r and D_s

Step 8: Determine the plant range and update the best search as D

Step 9 : $w=w+1$

Step 10: Return the best duty cycle value in accordance with GMPP.

Step 11: Finish

For further illustration, the flowchart of the algorithm is shown in Figure 2.

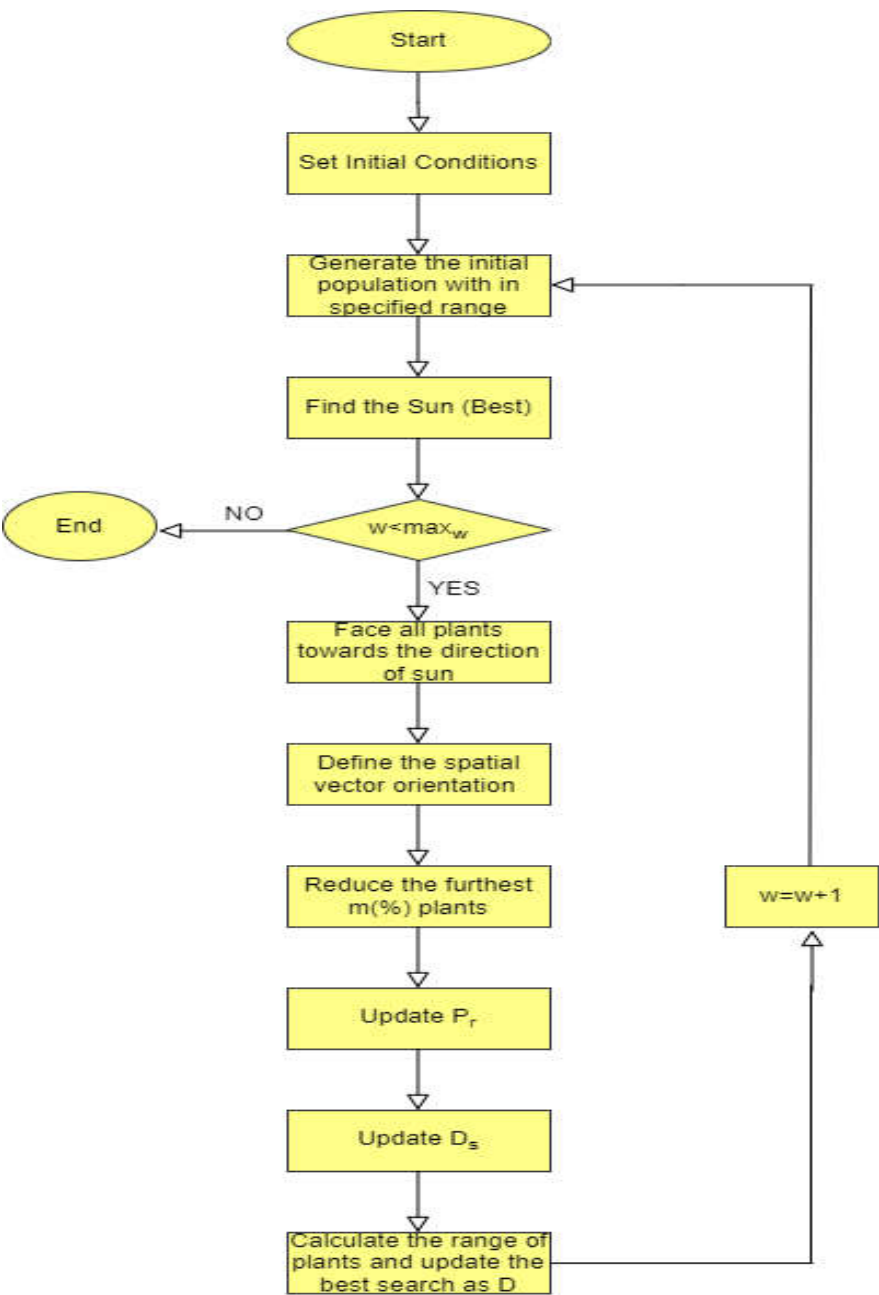


FIGURE 2 Flowchart for ASF algorithm

4. SIMULATION RESULTS

Matlab simulink tools have been used to simulate a 30kW, two-stage, three-phase grid-connected photovoltaic system using the ASF MPPT algorithm in the MATLAB/Simulink environment. When P_{limit} is reached or exceeded, ASF can limit power generation. The performance of the traditional P&O algorithm and the incremental conductance algorithm is then compared in terms of inverter output voltage, as shown in Figure 3.

Inverter Output Voltage Level to Grid

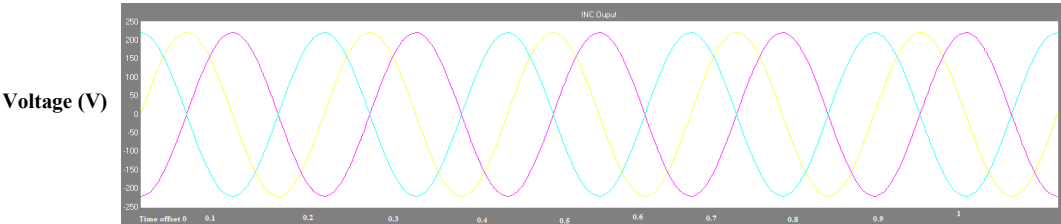


Figure3a. Grid phase voltage level using Incremental Conductance

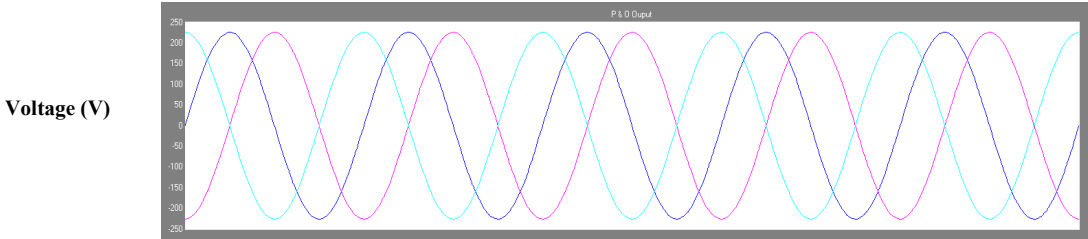


Figure3b. Grid phase voltage level using P&O

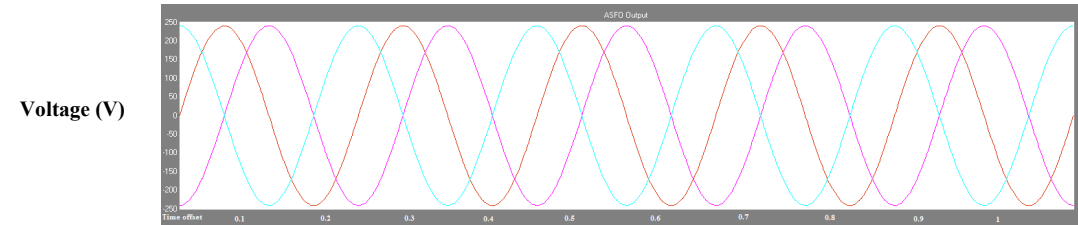


Figure3c. Grid phase voltage level using ASFO

Table 1 Grid Phase Voltage Level Summary

| Algorithms | Grid Phase Voltage Level |
|-------------------------|--------------------------|
| Incremental Conductance | 220V |
| P&O | 230V |
| ASF | 240V |

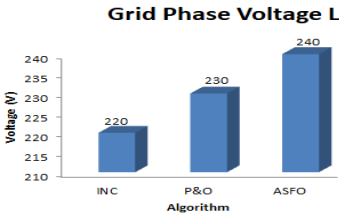


Figure3d. Grid phase voltage level comparison

The proposed algorithm provides the proper operating point direction toward the MPP as well as small voltage changes. Excess power is reduced by the ASF MPPT algorithm. At the same time, as the irradiation dose increases, so does the duty cycle. Conversely, as the irradiation dose decreases, so do the current and the duty cycle corresponding to the input voltage increases. Changes in DC stage voltage, phase voltage, and current exposure are depicted in Figure 4.

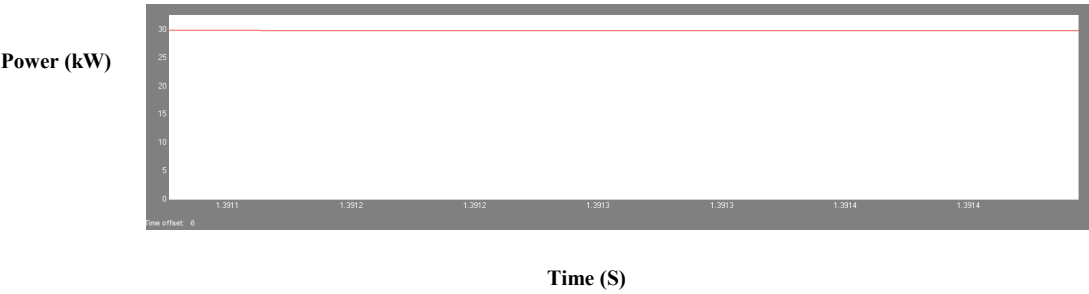


Figure4a. Power output from PV system



Figure4b. Grid voltage

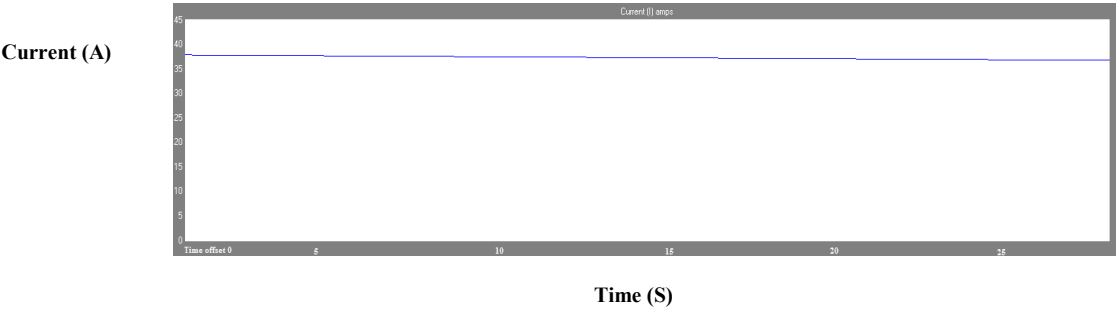


Figure4c. Grid current

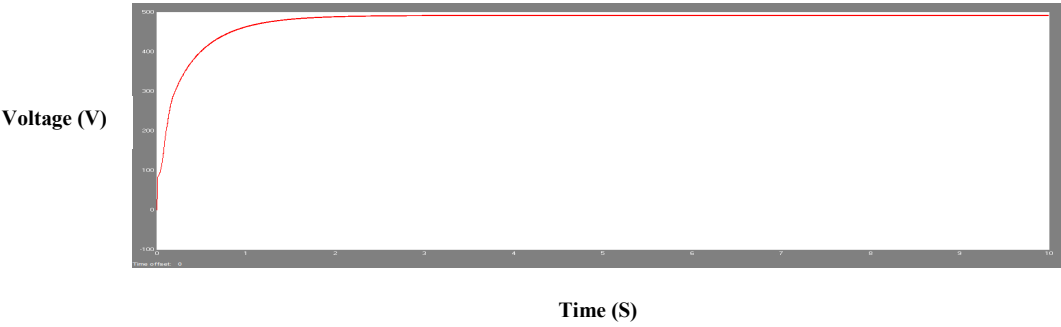


Figure4d. Boost output voltage

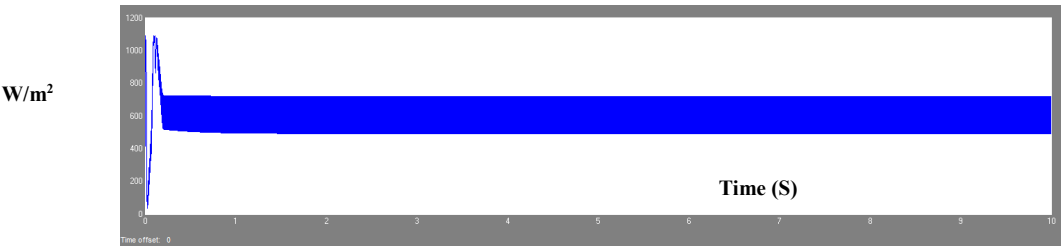


Figure4e. Irradiance variation

Figure 5 depicts the torque and speed curves. It quivers around the nominal value when the solar radiation and temperature values are optimal. A reduction in the irradiation and temperature profiles causes the torque to fall below the nominal value.

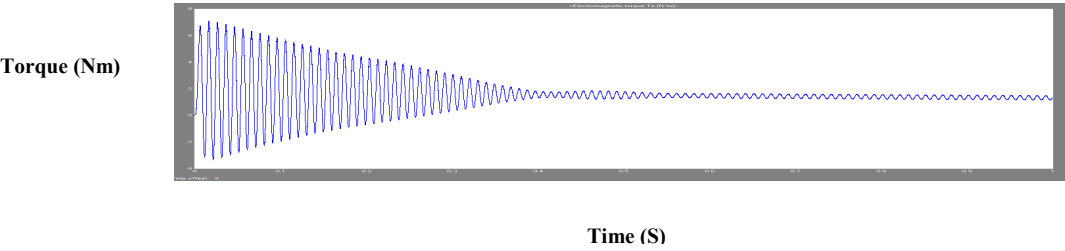


Figure 5a. Electromagnetic torque

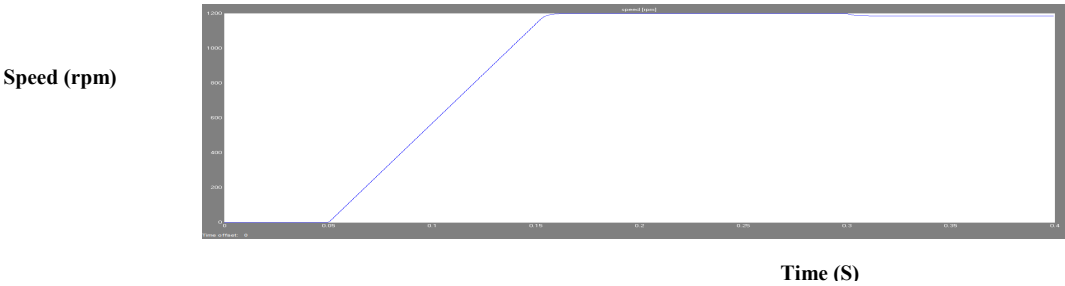


Figure 5b. Speed curve

PERFORMANCE ANALYSIS

Table 2 also includes a static performance analysis of the proposed ASF algorithm, existing P&O algorithms, and incremental conductance algorithms. The standard deviation is denoted by SD. The static analysis is expressed as the mean and SD of the settling time satisfying the VMPP. In this regard, 30 tests were carried out to evaluate the algorithm's performance under planned and variable survey conditions. The tests were performed with a constant irradiation of 700 W/m², i.e. $t = 6$ s. Under variable irradiation conditions, it goes from 700W/m² to 500W/m² and back to 500W/m² to 700W/m² from $t=3$ s to $t=1.5$ s. Table 3 clearly displays the process results in terms of mean settling time and standard deviation. The proposed algorithm outperforms the P&O algorithm and the incremental conductance on average. The results demonstrate the proposed ASF high robustness and search ability.

Table 2 Performance Analysis

| Irradiance Condition | Evaluation Parameter | Mean and SD | IC | P& O | Adaptive SFO |
|---|----------------------|-------------|--------------------------|---------------------------|---|
| Constant (700W/m ²) | $t_s V_{MPP}$ | Mean | 0.712 | 0.62 | 0.418 |
| | | SD | 1.1291×10^{-16} | 2.2981×10^{-16} | 2.5181×10^{-16} |
| Variable Condition (700 to 500W/m ²) | $t_s V_{MPP}$ | Mean | 1.7665 | 0.566 | 0.411 |
| | | SD | 1.14 | 0.0313 | 0.05237793 |
| Variable Condition (500 to 700 W/m ²) | $t_s V_{MPP}$ | Mean | 3.125 | 1.588 | 0.895 |
| | | SD | 0.00612587 | 4.55626×10^{-16} | 4.75626×10^{-16} |

5. CONCLUSION

The three-phase grid-connected photovoltaic system works in two stages to reduce the rated power of the equipment in generating mode and the extra power during peak hours. It also eliminates drift in existing P&O and incremental conductance algorithms. Furthermore, the algorithm operates in an improved MPPT mode with a shorter usage time. MPPT retains current information in this mode to distinguish changes in the survey. As a result, during irradiance changes, the search direction towards the MPP can be estimated. As a result, the operating point does not deviate from the MPPT's shortest path. The system was implemented for 30kW, 2-step, 3-phase GCPVS and Simpower tools were used to simulate it in the MATLAB/Simulink environment. The system performance demonstrates that the proposed algorithm actively contributes to energy savings during maximum generation time. The results also show that the improved algorithm responds faster than the existing P&O and incremental algorithms under various conditions.

REFERENCES

- [1] Sun, K., Yao, W., Fang, J. K., Ai, X. M., Wen, J. Y., and Cheng, S. J. Impedance modeling and stability analysis of grid-connected DFIG-based wind farm with a VSC-HVDC. IEEE J. Emerg. Sel. Top. Power Electron. 8, pp.1375–1390, 2020.
- [2] Song, D. R., Fan, X. Y., Yang, J., Liu, A. F., Chen, S. F., and Joo, Y. H. Power extraction efficiency optimization of horizontal-axis wind turbines through optimizing control parameters of yaw control systems using an intelligent method. Appl. Energy 224, pp.267–279, 2018.
- [3] Yang, B., Yu, T., Shu, H. C., Zhang, Y. M., Chen, J., Sang, Y. Y., et al. Passivity-based sliding-mode control design for optimal power extraction of a PMSG based variable speed wind turbine. Renew. Energy 119, pp.577–589, 2018b.
- [4] Peng, X. T., Yao, W., Yan, C., Wen, J. Y., and Cheng, S. J. Two-stage variable proportion coefficient based frequency support of grid-connected DFIG-WTs. IEEE Trans. Power Syst. 35, pp.962–974, 2020.
- [5] Song, D. R., Zheng, S. Y., Yang, S., Yang, J., Dong, M., Su, M., et al. Annual energy production estimation for variable-speed wind turbines at high-altitude sites. J. Mod. Power Syst. Clean Energy, 2020.
- [6] Yang, B., Yu, T., Shu, H. C., Dong, J., and Jiang, L. Robust sliding-mode control of wind energy conversion systems for optimal power extraction via nonlinear perturbation observers. Appl. Energy 210, pp.711–723, 2018a.
- [7] Zhang, H. X., Lu, Z. X., Hu, W., Wang, Y. T., Dong, L., and Zhang, J. T. Coordinated optimal operation of hydro-wind-solar integrated systems. Appl. Energy 242, pp.883–896, 2019.
- [8] Li, G. D., Li, G. Y., and Zhou, M. (Model and application of renewable energy accommodation capacity calculation considering utilization level of interprovincial tie-line. Prot. Control Mod. Power Syst. 4, pp1–12, 2019.

- [9] Zhang, X. S., Xu, Z., Yu, T., Yang, B., and Wang, H. (2020). Optimal mileage based AGC dispatch of a GenCo. *IEEE Trans. Power Syst.* 35, pp.2516–2526,2020.
- [10] Yang, B., Jiang, L., Wang, L., Yao, W., and Wu, Q. H. Nonlinear maximum power point tracking control and model analysis of DFIG based wind turbine. *Int. J. Electr. Power Energy Syst.* 74, pp.429–436,2016.
- [11] He, X., Ai, Q., Qiu, R. C. M., Huang, W. T., Piao, L. J., and Liu, H. C. A big data architecture design for smart grids based on random matrix theory. *IEEE Trans. Smart Grid* 8, pp.674–686,2017.
- [12] Xiao W, Edwin F, Spagnuolo G, Jatskevich J., Efficient approaches for modeling and simulating photovoltaic power systems, 2013
- [13] Tanvir A, Sharmin S, Faysal N., Comparative analysis between single diode and double diode model of PV cell: concentrate different parameters effect on its efficiency, 2016
- [14] R. Tonkoski, L. A. C. Lopes, and T. H. M. El-Fouly, “Coordinated active power curtailment of grid connected pv inverters for overvoltage prevention,” *IEEE Transactions on Sustainable Energy*, vol. 2, pp. 139-147, 2011.
- [15] W. A. Omran, M. Kazerani, and M. M. A. Salama, “Investigation of methods for reduction of power fluctuations generated from large grid connected photovoltaic systems,” *IEEE Transactions on Energy Conversion*, vol. 26, pp. 318-327, 2011.
- [16] Q. Zeng, L. Chang, P. Song, “SVPWM-based current controller with grid harmonic compensation for three-phase grid-connected VSI,” *IEEE 35th Annual Power Electronics Specialists Conference (PESC 04)*, Vol.4, pp.2494–2500, 2004
- [17] M. P. Kazmierkowski and L. Malesani, “Current Control Techniques for Three-Phase Voltage-Source PWM Converters: A survey,” *IEEE Trans. Ind. Electron.*, vol. 45, pp. 691-703, 1998.
- [18] IEEE Recommended Practice for Utility Interface of Photovoltaic (PV) systems, IEEE Standard 929-2000, 2000.
- [19] Zhou dejia,Zhao Zhengming; Eltawil, Mohamed; Yuan, Liqiang ,“Design and control of a three-phase grid-connected photovoltaic system with developed maximum power point tracking,” *IEEE Applied Power Electronics Conference and Exposition, APEC*, pp. 973-979, 2008.
- [20] Schonardie, Mateus F. Martins, Denizar C. ,“Three-phase grid-connected photovoltaic system with active and reactive power control using dq0 transformation,” *IEEE 39th Annual Power Electronics Specialists Conference*, pp. 1202-1207, 2008.
- [21] Zhou Dejia,Zhao Zhengming,Yuan Liqiang,Feng Bo,Zhao Zhiqiang ,“Photovoltaic grid-connected system based on a synchronous current vector PI controller,” *J Tsinghua Univ (Sci &Tech)*, Vol.49, No.1, pp. 33-36,2009.